

Tangential Intensity Algorithm for Acoustic Centering

Daniel Deboy¹, Franz Zotter²

¹ Student, KU-Graz, Email: daniel.deboy@student.kug.ac.at

² Institut für Elektronische Musik und Akustik, KU-Graz, Email: zotter@iem.at

Introduction

Today, the reproduction or synthesis of musical instruments has reached an acceptable level of authenticity in terms of timbre and temporal behavior. However, common loudspeaker systems are not designed to reproduce the radiation patterns of musical instruments since they always impose their own radiation characteristics. Spherical loudspeaker arrays were developed to fulfill this task and to take the step to a highly authentic reproduction including the instruments' directional information.

To obtain recordings of this information, surrounding microphone arrays have recently been constructed. They collect sound pressure signals simultaneously on various points on a sphere surrounding the instrument. These signals can be converted to spherical harmonic components for interpolation. Hereby, also other manipulation is enabled, e.g. changing the orientation of the instrument.

Spatial shifts of the instrument during recording, or a decentralized acoustic location evoke higher order components, which often cannot be reproduced on low-order playback devices. Recently, algorithms to acoustically center a decentralized instrument have been investigated. Due to their high complexity, they are currently applicable only for offline computation.

In this paper, we investigate a new approach using tangential acoustic intensities. The tangential intensity can be derived from sound pressure signals and indicates decentralization. Low computational effort and easy implementation as an iterative gradient algorithm make it promising for realtime applications like "teleportation" of musical performances from one space to another.

Radial and Tangential Intensity

The IEM surrounding microphone array has 64 sampling nodes located on a sphere. The goal is to develop an acoustic centering [2] algorithm for sound sources within such an array. Thus, we derive the acoustical intensities on a sphere and discretize later on to the sampling nodes.

The acoustical intensity is defined using the sound pressure p and the velocity \mathbf{v}

$$\mathbf{I} = \frac{1}{2} \Re\{p^* \mathbf{v}\}. \quad (1)$$

The Euler equation gives the relation between pressure and velocity,

$$\mathbf{v}(\omega) = -\nabla \frac{p(\omega)}{i\omega\rho}. \quad (2)$$

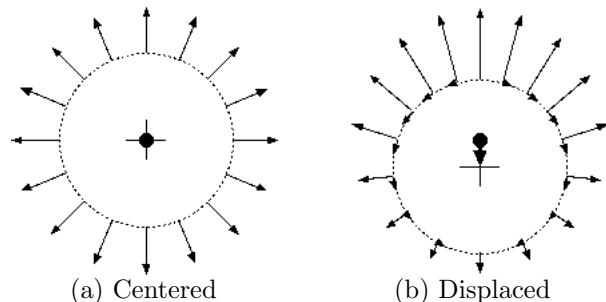


Figure 1: In a) an omnidirectional source lies in the origin of the microphone array. In this case, the Intensity on the surface has no tangential components. In b) the source has been displaced from the origin, the Intensity now also has tangential components \mathbf{I}_θ on the array surface.

Given an angular unit vector $\boldsymbol{\theta}$ on a sphere with the radius r , the intensity can be split up into a radial and a tangential component, using inner and cross products,

$$I_r(\boldsymbol{\theta}) = \mathbf{I}^T \boldsymbol{\theta}, \quad \mathbf{I}_\theta = \mathbf{I}^T \left(\frac{\mathbf{I} \times \boldsymbol{\theta}}{\|\mathbf{I} \times \boldsymbol{\theta}\|} \times \boldsymbol{\theta} \right). \quad (3)$$

Integrating the radial intensity over the angles of the spherical surface yields the radiated power of enclosed sources. In addition to that, we propose the integral over the tangential components to estimate the displacement of the source, cf. Fig. 1,

$$\Pi = r^2 \int_{\mathbb{S}} I_r d\boldsymbol{\theta}, \quad \hat{\mathbf{d}} \propto \frac{r^2 \int_{\mathbb{S}} \mathbf{I}_\theta d\boldsymbol{\theta}}{\Pi}. \quad (4)$$

The estimation of a *wave spectrum* as given in [2] provides the required information to estimate the intensities from data measured on a sphere as it estimates the sound field analytically. If external sources/reflections are absent and the radiator has a finite order N , the *exterior problem* remains with the radiating components

$$p(kr, \boldsymbol{\theta}) = \sum_{n=0}^N \sum_{m=-n}^n c_n^m h_n^{(2)} Y_n^m(\boldsymbol{\theta}), \quad (5)$$

where c_n^m is the estimated wave spectrum, $h_n^{(2)}$ are the spherical Hankel functions, and Y_n^m are the spherical harmonics. The tangential derivative can be expanded into spherical harmonics given the coefficients $\mathbf{g}_{nn'}^{mm'}$ of the differentiation theorem, cf. [4]

$$\nabla p(kr, \boldsymbol{\theta}) = \sum_{n=0}^{N+1} \sum_{m=-n}^n \left[\sum_{n', m'} \mathbf{g}_{nn'}^{mm'} c_{n'}^{m'} \right] h_n^{(2)} Y_n^m(\boldsymbol{\theta}). \quad (6)$$

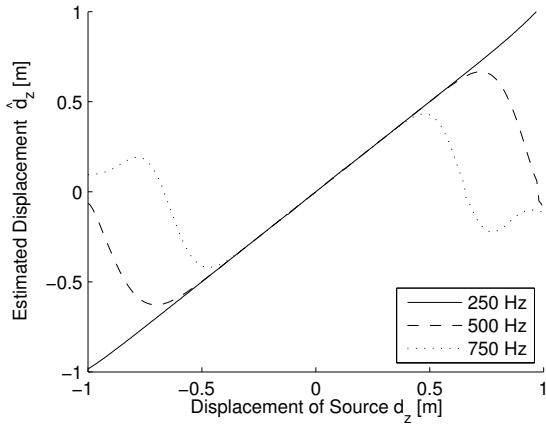


Figure 2: An omnidirectional source is shifted along an arbitrary axis z , the resulting estimator $\hat{\mathbf{d}}$ is linear proportional to the displacement \mathbf{d} .

The radiated power Π is derived from the wave spectrum by the Euler equation and the radial components, cf. [1],

$$\Pi = \frac{1}{2\rho ck^2} \mathbf{c}_N^H \mathbf{c}_N. \quad (7)$$

The three components of the displacement estimator can also be obtained from the wave spectrum, denoting the corresponding values of $h^{(2)}$ as a matrix \mathbf{H} and the differentiation coefficients as a matrix $\mathbf{G}_{\{x,y,z\}}$,

$$\hat{\mathbf{d}}_{\{x,y,z\}} \propto \frac{r^2}{2i\omega\rho} \frac{\Re\{\mathbf{i}(\mathbf{H}_N \mathbf{c}_N)^H \mathbf{G}_{\{x,y,z\}} \mathbf{H}_N \mathbf{c}_N\}}{\Pi}. \quad (8)$$

In the following section we will investigate if this resulting estimator $\hat{\mathbf{d}}$ is proportional to the real displacement vector \mathbf{d} of an omnidirectional source.

Centering An Omnidirectional Source

In fig. 2 the length of the resulting vector $\hat{\mathbf{d}}$ scaled with a factor which has been estimated empirically is plotted against the displacement vector \mathbf{d} of a simulated omnidirectional source along an arbitrary axis z . Within a certain, frequency dependent radius both values are linearly proportional. The limitation is caused by spatial aliasing which occurs if higher order components arise due to the displacement [2].

In the following examples, the resulting vector has been scaled with the mean value of the ratio d_z/\hat{d}_z . Displacements of the omnidirectional source have been made in 10 cm steps from 10 to 50 cm. In fig. 3 a) the absolute error is plotted for different frequencies. For a rough comparison with real world data, a loudspeaker in a small enclosure has been placed with the same displacements in the IEM array. As excitation signal, an exponential frequency sweep was used. Fig. 3 b) shows the results.

Both, the simulation and the measured data, have in common a decreasing performance at higher frequencies due to spatial aliasing. At low frequencies the simulated source still gives good results whereas the loudspeaker doesn't. Possible reasons are the poor performance of the room and the loudspeaker at low frequencies.

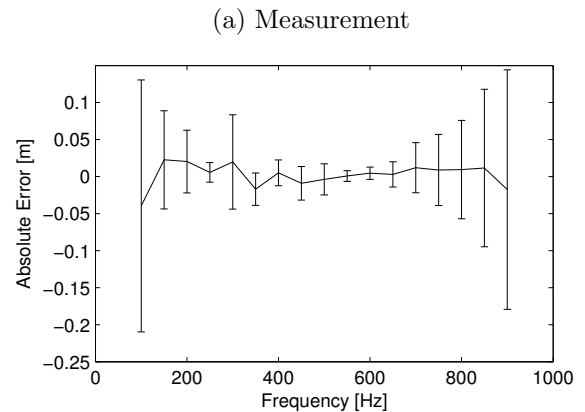
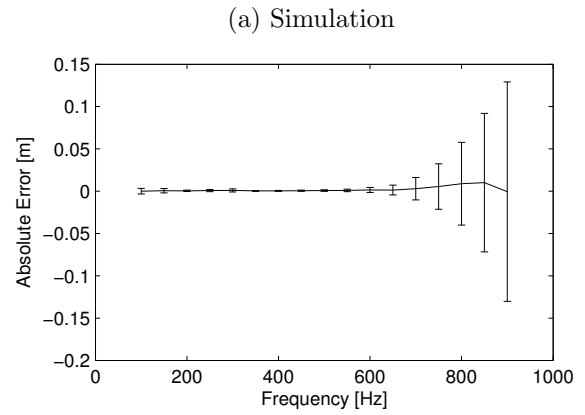


Figure 3: Mean error of the resulting estimator $\hat{\mathbf{d}}$ for source displacements of 10 to 50 cm.

Conclusion

The sum of tangential intensity components on a surrounding microphone array yield a resulting vector which is linear proportional to the displacement of an omnidirectional sound source and thus may be used for algorithmic centering of the source. However, if the displacement exceeds a frequency dependent radial limit, spatial aliasing evokes distortion which may render the resulting vector useless for centering.

In comparison to centering algorithms we recently proposed, c.f. [2], the computational effort may reduce dramatically if using the proposed estimator $\hat{\mathbf{d}}$, since no optimization in the spherical volume of the array is needed to obtain an estimate of the displacement vector.

In future studies, the influence of higher order components of sources has to be investigated.

References

- [1] E. Williams: Fourier Acoustics. Academic Press, 1999.
- [2] D. Deboy: Acoustic Centering and Rotational Tracking in Surrounding Spherical Microphone Arrays. M. Thesis, KU Graz, 2010.
- [3] F. Zotter: Analysis and Synthesis of Sound-Radiation with Spherical Arrays, Dissertation Thesis, KU Graz, 2009.
- [4] W. C. Chew: Recurrence Relations for Three-Dimensional Scalar Addition Theorem. J. Electromag. Waves and Appl., vol. 6, no. 2, 1992.